Calibration Model for Detection of Potential Demodulating Behaviour in Biological Media Exposed to RF Energy

See, CH, Abd-Alhameed, RA, Ghani, A, Ali, N, Excell, P, McEwan, NJ & Balzano, Q

Original citation & hyperlink:
See, CH, Abd-Alhameed, RA, Ghani, A, Ali, N, Excell, P, McEwan, NJ & Balzano, Q 2017, 'Calibration Model for Detection of Potential Demodulating Behaviour in Biological Media Exposed to RF Energy' *IET Science, Measurement and Technology*, vol 11, no. 7, SMT-2017-0105, pp. 900-906
https://dx.doi.org/10.1049/iet-smt.2017.0105

DOI 10.1049/iet-smt.2017.0105
ISSN 1751-8822
ESSN 1751-8830

Publisher: IEEE

Research Article

Calibration model for detection of potential demodulating behaviour in biological media exposed to RF energy

Chan H. See[1,2] ✉, Raed A. Abd-Alhameed[2], Arfan Ghani[3], Nazar T. Ali[4], Peter S. Excell[2,5], Neil J. McEwan[2,5], Quirino Balzano[6]

[1]*School of Engineering, University of Bolton, Deane Road, Bolton, BL3 5AB, UK*
[2]*Antennas and Applied Electromagnetics Research Group, University of Bradford, Bradford, BD7 1DP, UK*
[3]*School of Computing, Electronics and Mathematics, Coventry University, CV1 5FB, UK*
[4]*Khalifa University of Science, Technology and Research (KUSTAR), Sharjah, UAE*
[5]*Wrexham Glyndwr University, Wrexham, LL11 2AW, UK*
[6]*Department of Electronic and Computer Engineering, University of Maryland, College Park MD, USA*
✉ *E-mail: c.see@bolton.ac.uk*

Abstract: Potential demodulating ability in biological tissue exposed to radio-frequency (RF) signals intrinsically requires an unsymmetrical diode-like non-linear response in tissue samples. This may be investigated by observing possible generation of the second harmonic in a cavity resonator designed to have fundamental and second harmonic resonant frequencies with collocated antinodes. Such a response would be of interest as being a mechanism that could enable demodulation of information-carrying waveforms having modulating frequencies in ranges that could interfere with cellular processes. Previous studies have developed an experimental system to test for such responses: the present study reports a circuit model to facilitate calibration of any non-linear RF energy conversion occurring within a test-piece inside the cavity. The method is validated computationally and experimentally using a well-characterised non-linear device. The proposed model demonstrates that the sensitivity of the measurement equipment plays a vital role in deciding the required input power to detect any second harmonic signal, which is expected to be very weak. The model developed here provides a lookup table giving the level of the second harmonic signal in the detector as a function of the input power applied in a measurement. Experimental results are in good agreement with the simulated results.

1 Introduction

With the rapid growth of mobile communication usage over recent decades, public concerns have been raised about the possible biological effects of non-ionising radiation with specific regard to radio-frequency (RF) radiation from mobile phones [1, 2]. The possible effects of this radiation can be categorised into two groups: thermal effects resulting from high-level RF power and putative non-thermal effects due to low power radiation. Thermal effects of RF radiation have been extensively studied by many researchers and are well understood and uncontroversial [1, 2]; in contrast, non-thermal effects of such radiation are still debated by many scientists, with conflicting arguments still being presented. As a result, intensive effort worldwide continues to develop research in aspects of bioelectromagnetics at macroscopic and microscopic levels. This has led to different defined levels of analysis, i.e. human level, tissue level, cell level and ionic level [3–22].

From the published literature [1–7], it may be observed that many of the works have treated RF and tissue interaction mechanism effects as a linear problem. Relatively few papers [8–13] have moved towards searching for proof of the existence of non-linear biological tissue responses, including molecular processes and microscopic studies at cellular level. These studies are typically either theoretical or experimental, the latter covering molecular, cellular or tissue-level experiments or else statistical studies of whole-organism effects in human or animal cohorts. Recently, Balzano *et al*. [8–11] has proposed novel experiments to detect the presence of asymmetrical (rectifying) non-linear interactions at cellular or tissue-sample level, under exposure by low-amplitude RF carrier signals. These build on the observation that demodulation of a modulated carrier inherently requires such asymmetrical behaviour and this would necessarily cause the production of second harmonics. Such demodulation has been postulated as a plausible mode for putative non-thermal effects of RF radiation on any contiguous living system.

Balzano's proposals adopted the concept of an ingenious doubly-harmonic resonant cylindrical cavity model having co-located antinodes at fundamental and second harmonic frequencies [8–11]: the paper presented here develops an electric circuit mathematical model to link the cavity model with second harmonic generation from a given non-linear device. The results can be used to indicate the amount of input power needed to stimulate the biological sample in order to maximise the likelihood of detecting any second harmonic reradiation.

2 Methodology

The proposed mathematical model is an extension of some of the authors' earlier work [23, 24]. It consists of two parts: cavity model and electric circuit model: in addition, experimental verification was undertaken. In the cavity model, the electric field distributions were studied at TE_{111} and TE_{113} modes. Following this, the cavity model was used to extract its *S*-parameters by using CST Microwave Studio [25] and ANSYS HFSS [26] software. Once these data were obtained, they could be adopted into the derived equations from the proposed circuit model to compute the second harmonic power level with a given input power.

2.1 Cavity model and electric fields analysis

The previously-reported practical work [13] was undertaken with an RF carrier frequency in the 880–890 MHz band. To examine whether biological tissues exhibit unsymmetrical non-linearity when exposed to RF signals in this band, an efficient and high quality-factor dual-resonant cylindrical cavity with height 272 mm

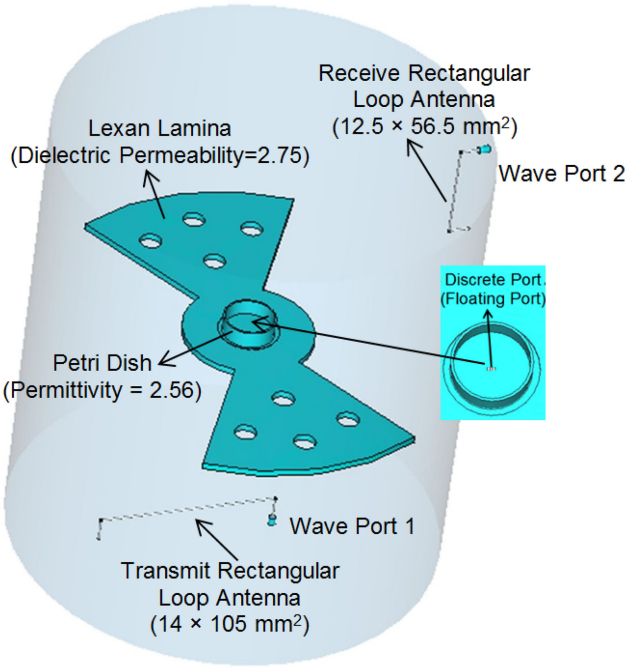

Fig. 1 *Dimensions of the cavity model, with two rectangular loop antennas and Lexan sample support structure*

and diameter 248 mm was used, based on Balzano's proposals [8, 10, 11]. Fig. 1 shows the cavity structure, including two loop antennas (for fundamental input and second-harmonic output) and a biosample support structure consisting of a butterfly-shaped Lexan lamina (polycarbonate) [11] and a Petri dish [27]. This supporting structure is designed to minimise dielectric loss in the cavity, other than the energy dissipation in the biosample. Lexan is practically lossless at the frequencies of operation of the cavity and has a relative dielectric permeability of between 2.5 and 3.0. The holes in the lamina were added to decrease the overall dielectric loading of the cavity. The central circle in the lamina has a 1 mm depression to hold a 3.5 cm diameter Petri dish centrally.

Loop antennas were selected for coupling because they couple with both H_Φ (the azimuthal magnetic field) and E_r (the radial electric field) and thus have a much wider reactive matching range than a monopole [8]. The cavity is excited by a loop antenna with dimensions of 14×105 mm located in the middle of the bottom plate, the dimensions corresponding to a total length of 0.4 λ at 882 MHz. This acts as a transmitter to excite the TE_{111} cavity mode in the frequency range of 880–890 MHz. The other antenna on the side wall of the cavity has dimensions of 12.5×56.5 mm, which is equivalent to length of 0.48λ at 1764 MHz (the second harmonic). This acts as a receiver to detect the energy of the TE_{113} cavity mode in the 1760–1790 MHz band, i.e. exactly double the input frequency. To maintain the highest sensitivity for detection of second harmonic responses, it is important to place both antennas at maxima of their corresponding operating modes, i.e. TE_{111} or TE_{113}. It is also essential to fine-tune the lengths of both antennas to achieve the resonance of the TE_{113} mode at exactly double the resonance frequency of the TE_{111} mode. To better understand these modes, Fig. 2 depicts the total electric field distributions for both modes. As can be seen, the TE_{111} mode has a maximum E-field in the centre of the cavity while the TE_{113} also has a field maximum at this point, plus others at $d/6$ and $5d/6$, where d is the height of the cavity.

To verify the accuracy of the predicted electric field intensity in the cavity model, computer simulation studies were undertaken to establish the maximum permissible input signal which will prevent to sample from reaching damaging levels of power dissipation. By using two different EM software packages (CST Microwave Studio and ANSYS HFSS), the field strength in the sample region as a function of input power was computed (Fig. 3). Two media samples were considered: air ($\varepsilon_r = 1$, $\sigma = 0$) and generic biological medium ($\varepsilon_r = 50$, $\sigma = 1$ S/m), with a volume of 60 µl. This 60 µl lossy medium was modelled as a cylindrical structure with diameter of 35 mm and height of 62.36 µm. The results, presented in Fig. 3, show that the biosample does not substantially alter the fields in the cavity, thus not degrading substantially its high Q that is necessary to detect weak second harmonic fields.

The International Commission on Non-Ionising Radiation Protection limit for SAR in functioning human tissue is 2 W/kg [28], which has been argued to include a large safety factor. The UK National Radiological Protection Board (NRPB) [29] formerly argued that its preferred limit of 10 W/kg was more realistic, although that would also include some safety factor: the NRPB has now become the Health Protection Agency and has adopted the internationally-agreed 2 W/kg limit. Because of this safety factor, plus the convection cooling that would occur in the cavity and the fact that a contiguous living organism is not involved in the tests, it was concluded that the option of going up to 100 W/kg should be available to the experiment. From the SAR equation, where $\text{SAR} = \sigma E_{\text{peak}}^2/2\rho$, E_{peak} can be found for a specified value of SAR. $\sqrt{(2\rho \times \text{SAR})/\sigma}$ Taking SAR = 100 W/kg as the upper limit and using the properties of pure water at this frequency, $\rho = 1000$ kg/m^3 and $\sigma = 1$ S/m, as reasonable approximations for biological tissue, it is found that $E_{\text{peak}} = 447$ V/m. This field strength applies within the sample, and the value outside could be higher, depending on its orientation. This indicates that a maximum power of the order of 250 mW (from Fig. 3) must be the limit for the experiment.

2.2 Electric circuit model for calibrations

A mathematical technique was developed to compute the second harmonic power with a known input power in the presence of a known unsymmetrical non-linear device in the Petri dish. This method enables more precise quantification of the amount of input power required in the excitation port in order to generate a detectable second harmonic signal. An outline of the method has been published elsewhere [24], although without verification test results, and hence it is given in summary form here.

For derivation of the required formulae, the cavity model used in the previous study [11–13] was adopted. Then, a discrete floating port with dipole structure, having metal leads 1 mm long, is considered to be placed in the centre of the Petri dish in the cavity and oriented parallel to the transmit antenna, as illustrated in Fig. 1. This port receives the maximum RF signal from the transmit antenna. In order to extract the 3×3 Z-parameters at the two resonant frequencies of the TE_{111} and TE_{113} modes, two simulations were carried out, one for each mode and frequency. Based on this, an equivalent three-port network can be established, as shown in Fig. 4. From this network, two separate sets of 3×3 Z-parameters were found, one for each frequency: these were then applied in the three-port models shown in Figs. 4*a* and *b*. As can be seen in Fig. 4*a*, a diode is used as a well-characterised unsymmetrical non-linear element in the Petri dish in the cavity, its leads constituting the dipole arms, while the input and output ports can be represented as transmit and receive antennas, respectively. Fig. 4*a* depicts the equivalent electric circuit of the diode model. It should be noted that Fig. 4 was drawn by the electrical circuit symbols from Keysight ADS [30].

By applying Ohm's law to the circuits in Fig. 4*a*, a matrix equation can be derived.

$$[\boldsymbol{V}] = [\boldsymbol{Z}][\boldsymbol{I}] \tag{1}$$

where $[\boldsymbol{V}] = [V_1\ V_2\ V_3]^{\text{T}}$ is a vector of port voltages, $[\boldsymbol{Z}]$ is a 3×3 symmetrical matrix of impedances and $[\boldsymbol{I}] = [I_1\ I_2\ I_3]^{\text{T}}$ is a vector of port currents.

The currents for the TE_{111} mode can be easily derived from the applied input voltage and the load/source impedances (these are equal to the characteristic impedance $Z_o = 50\ \Omega$ as shown in Fig. 4*a*). The $[\boldsymbol{Z}]$ matrix in this case is evaluated for the TE_{111} mode. It should be noted that the voltage (V_d) and the current (I_d) across the diode can be simply expressed by I_3 and V_3.

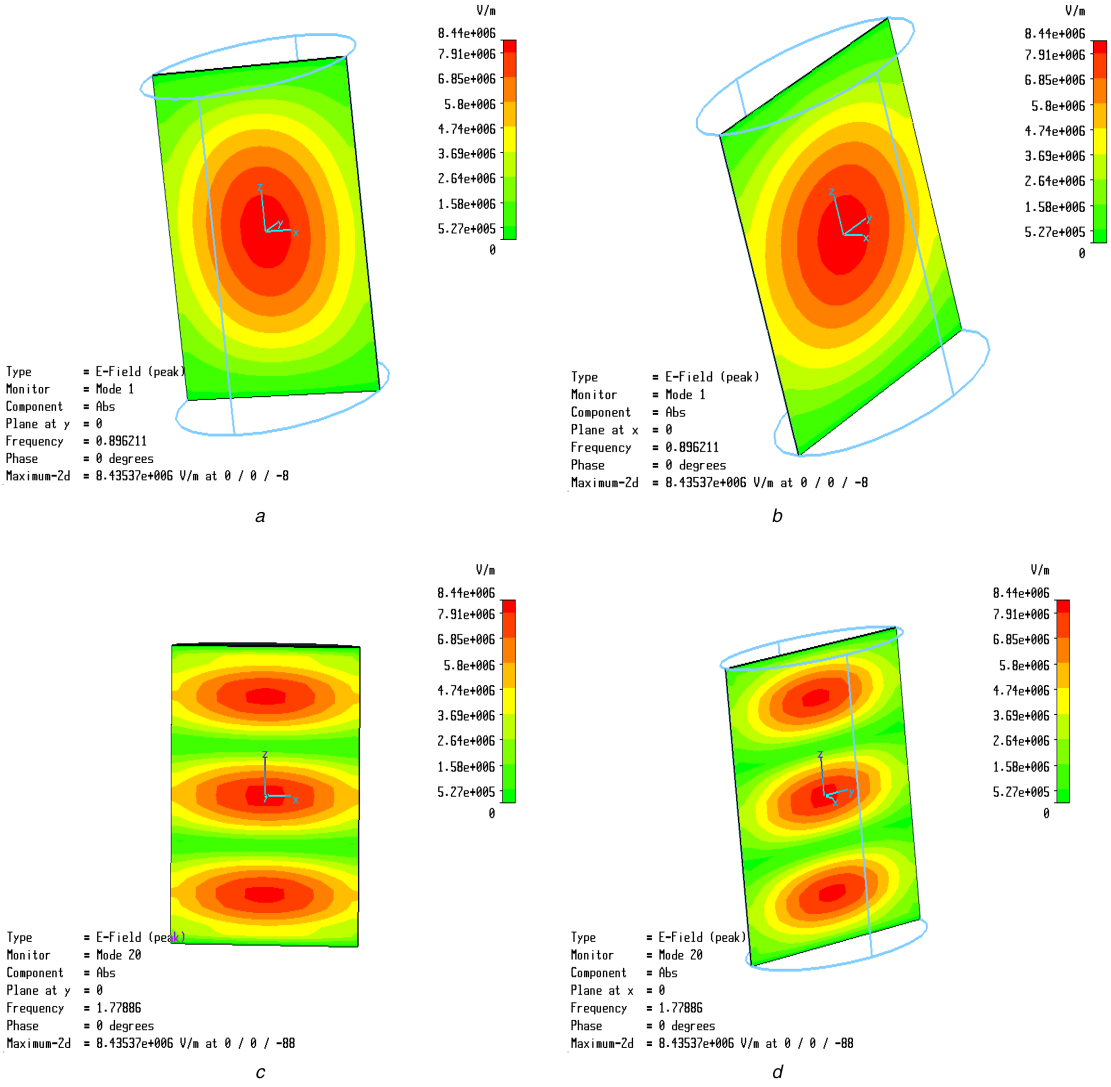

Fig. 2 *Electric fields distributions through the centre of the cavity*
(a) Total E-field of TE_{111} mode on *xz*-plane, ***(b)*** Total E-field of TE_{111} mode on *yz*-plane, ***(c)*** Total E-field of TE_{113} mode on *xz*-plane, ***(d)*** Total E-field of TE_{113} mode on *yz*-plane

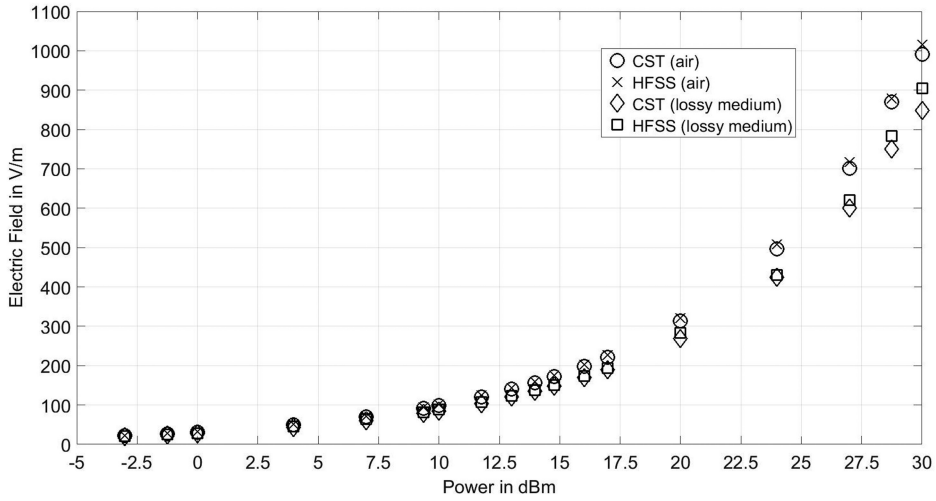

Fig. 3 *Electric field intensity in the cavity with and without presence of biological tissue, as computed by two different simulation packages*

For the diode parasitic components, values of $R_1 = 106.5\ \Omega$ and $C_1 = 1.5$ fF were adopted [31]; then (1), subject to input voltage V_i at port 1 can be established to compute V_d. Once V_d is found, it can be applied as the excitation source to the non-linear element. By substituting the Z-parameters of the TE_{111} mode into (1) and choosing a value for the input voltage, the parameters V_1, V_2 and V_d can be calculated. Then, the input power of the model can be calculated by $P_{in} = 0.5\ \mathrm{Re}(V_1 \times I_1)$.

The circuit in Fig. 4*a* was modified to apply to TE_{113} mode, as in Fig. 4*b*. By simple manipulation of the new voltage matrix elements, $[\boldsymbol{V}'] = \left[V_1' \quad V_2' \quad V_3'\right]^{\mathrm{T}}$ and applying the standard Shockley diode equation, the currents in the ports of the TE_{113}

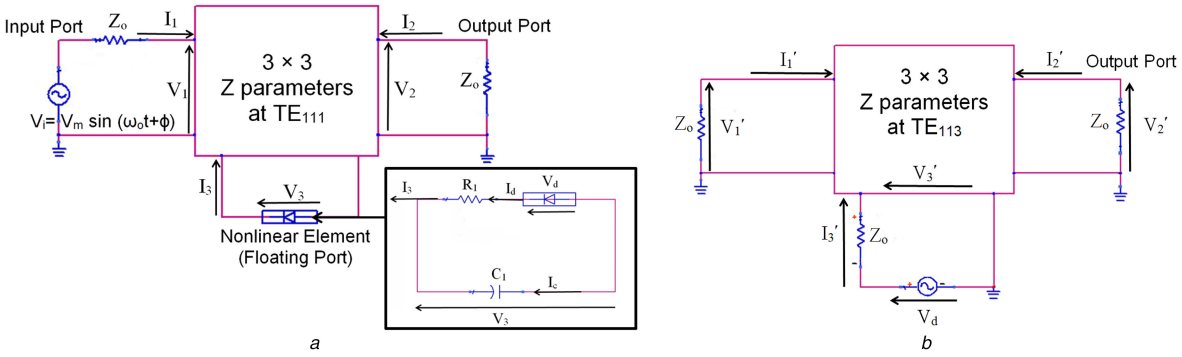

Fig. 4 *Three-port models for TE_{111} and TE_{113} modes of the cavity, including equivalent circuit of the non-linear element (diode)*

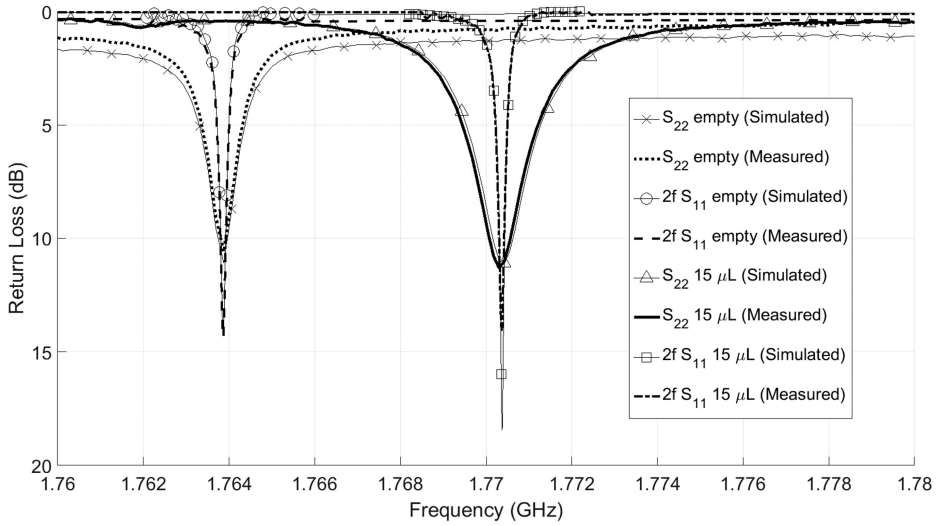

Fig. 5 *Fundamental and second harmonic responses of the loaded and unloaded cavity, showing simulated and measured results (fundamental frequency doubled for convenience of display purposes)*

mode of Fig. 4*b* can be found, and hence the output power on port 2 can be calculated by $P_{\text{out}} = 0.5\text{Re}(V_2' \times I_2'^{*})$.

3 Simulation results

Fig. 5 illustrates the reflection coefficients of the two antennas in the cavity found from simulations over the designed bands of operation: the dashed lines and solid lines represent the return losses of the antennas under unloaded and loaded tests. In the simulated unloaded test, an empty 3 cm Petri dish in the cavity was considered, while the loaded test added a 15 µl volume of deionised water, having properties $\varepsilon_r = 78.24$, $\sigma = 0.173$ S/m [4]. This formed a lamina of cylindrical shape in the bottom of the Petri dish inside the cavity. The purpose of the loaded test was to examine whether additional dielectric material introduced into the cavity, e.g. cells, tissue and/or medium, would result in any changes in resonant frequencies. In both test result graphs, the frequency fed to the transmitting antenna has been multiplied by a factor of two to enable direct comparison with second harmonic responses in the desired operating band. It is clear that both loaded and unloaded tests demonstrate that the antennas demonstrate reasonable reflection coefficients within spectrum bands covering both modes. Since a good margin of operational frequency of around 150 kHz at −10 dB reflection exists for both modes (i.e. both ports maintain good matching to 50 ohm loads). It is observed that when the cavity is loaded, the resonant frequency is slightly decreased for both modes, which continue to track each other in a 2 : 1 ratio.

4 Experimental validation

An experimental corroboration of the simulated results was derived from the equipment assembled to undertake the earlier tests on biological samples [12]: this comprised the dual mode ($TE_{111/113}$) cavity based on Balzano's proposals [8, 10, 11], with a sensitive measurement system based on an HP8510C vector network analyser. It may be observed that the simulated and measured results for return loss (Fig. 5) are in very good agreement. Slight discrepancies between the four sets of simulated and measured results can be attributed to uncertainties in the electrical properties of the materials used in the simulation model, the simplifications in the simulated structure and fabrication variations.

An important objective of the paper was a calibration curve giving the second harmonic power as a function of the input power as the input voltage was increased. This was initially computed using the model of the cavity based on CST software; however, in order to cross-validate the result, ANSYS HFSS software was also adopted for comparison [26]. The resulting curves are shown in Fig. 6, as can be seen, both simulation results were in excellent agreement.

To further validate this result, an experiment with a Schottky diode placed in the centre of the Petri dish in the cavity was set up as shown in Figs. 7 and 8. An Anritsu Synthesized Signal Generator MG3632A was used to generate the input signal to the bottom excitation antenna at 0.882 GHz. Two stages of low pass filters were used to suppress frequencies above 1 GHz, minimising any second harmonic products created by the input generator. On the output port, an Anritsu Spectrum Analyser MS2802A was set to display the expected second harmonic frequency component, at a minimum bandwidth of 1.764 GHz ± 100 kHz. High-pass and narrow band-pass filters were applied to the output to ensure at least −60 dB rejection of the fundamental frequency component. Comparing both predicted sets of results with the experimental ones, as shown in Fig. 6, it is observed that they are almost indistinguishable.

In addition, the variation of the second harmonic signal intensity against different lengths of the diode leads was also investigated experimentally. It should be noted that two

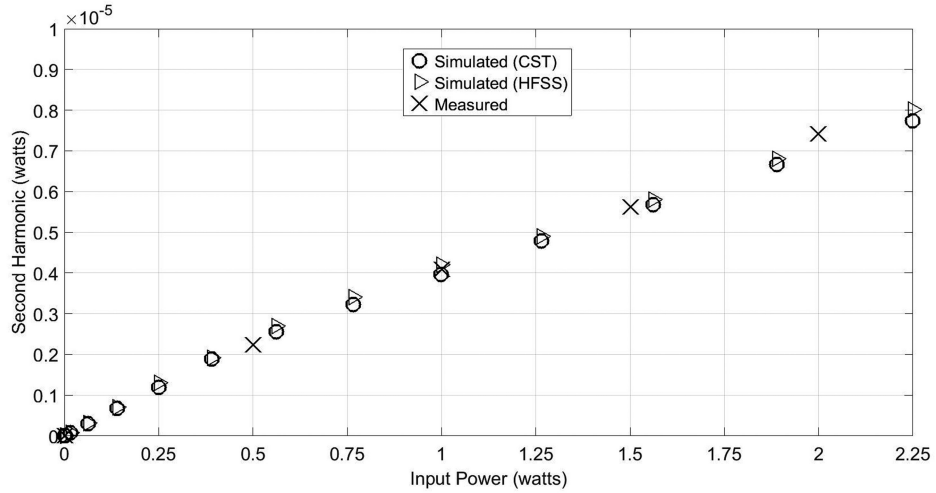

Fig. 6 *Input power at Port 1 versus second harmonic power at Port 2*

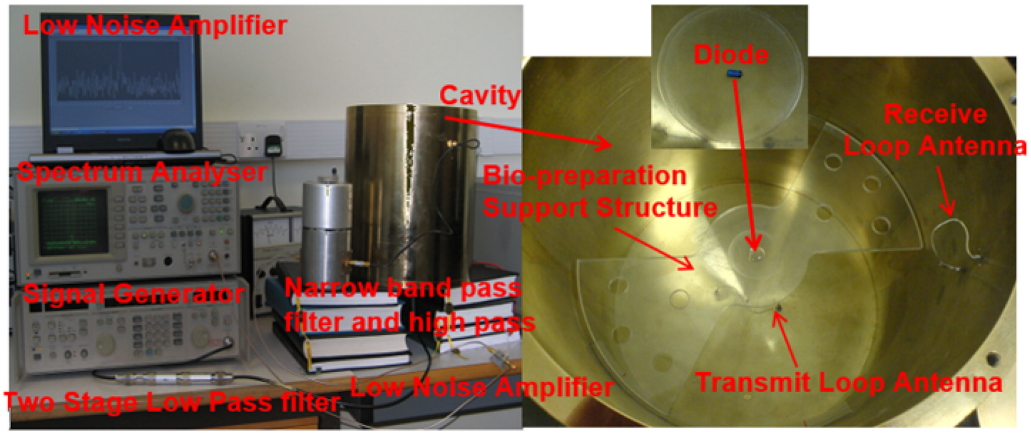

Fig. 7 *Experimental setup for validation test*

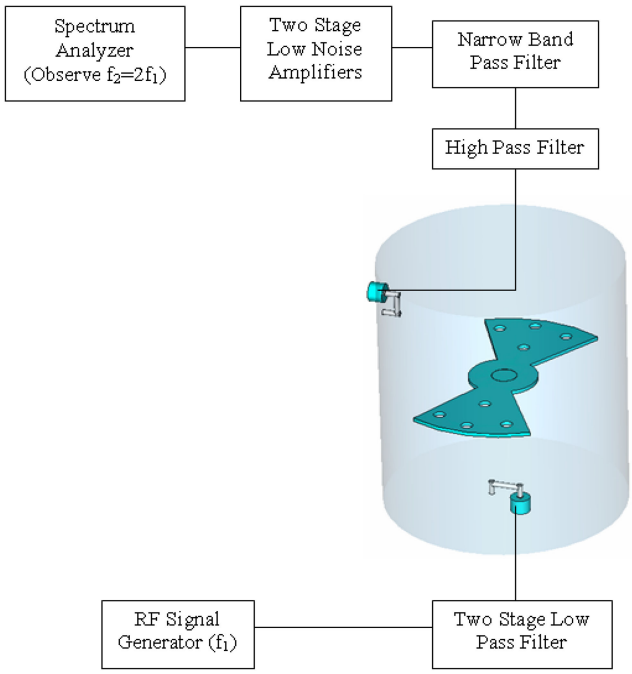

Fig. 8 *Block diagram for the experimental setup*

experimental setups were used, i.e. with and without the two stage low noise amplifiers shown in Fig. 8 (ZRL-2400 LN and Zel01724LN, from Mini-Circuits Inc.). The diode lead lengths were varied between 0 and 28 mm and placed into the middle of the dish inside the cavity: the diode body was 4 mm in length. The orientation direction was kept parallel to the transmit antenna at port 1. The results with and without amplifiers are shown in Figs. 9 and 10. These illustrate that as the length of the diode leads is reduced, the second harmonic signal strength is decreased, as expected.

As can be seen in the case without amplification, a minimum noise floor of −115 dBm was observed, and as the length of the diode leads gradually reduced from 28 to 0 mm, the second harmonic signal strength dropped down linearly from −58 to −108 dBm, corresponding to a difference between the noise floor and the second harmonic signal varying from 57 to 7 dBm. It is noticeable that the generation of the second harmonic by the diode without leads, is indistinguishable from the noise signal. However, when 60 µl of deionised water was added to the diode without leads, the second harmonic signal was improved from −108 to −95 dBm, i.e. 13 dBm enhancement in second harmonic power level.

When the amplifiers were used in the measurements, the noise floor of the spectrum analyser rose up to −100 dBm, as seen in Fig. 10. As can be seen, the second harmonic signal is raised to −62 dBm, and when the water was added a further increase of 20 dBm was observed (i.e. the second harmonic rose to −42 dBm). This strongly suggests that the presence of water acts as a return path for current, creating a distributed complete circuit which will act as a form of loop antenna and hence be much more effective than the short dipole antenna constituted by the diode leads alone. Since biological tissue is generally more conductive than pure water, this effect might be expected to be manifested more strongly, although a discrete single rectifying junction is not to be expected in any speculative theory of bioelectromagnetic interactions and hence any ‘loop antenna’ effect may be expected to be distributed throughout any sample

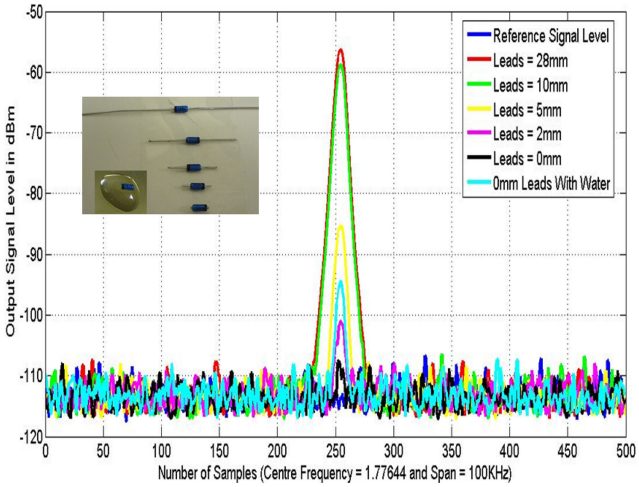

Fig. 9 *Output signal levels for detection system without amplification*

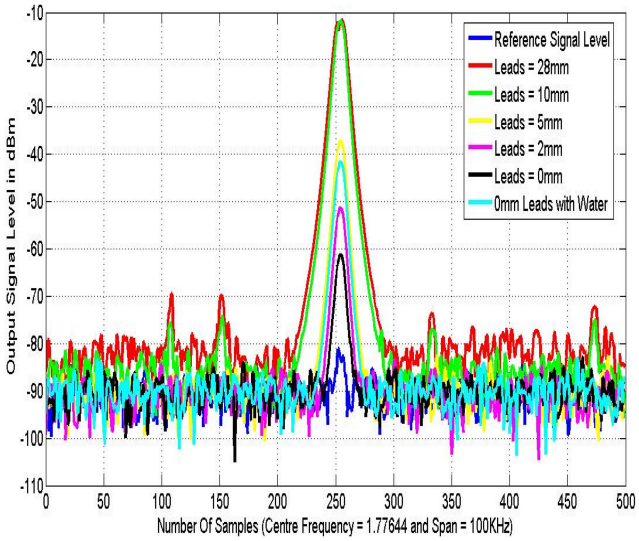

Fig. 10 *Output signal levels for detection system with amplification*

5 Conclusion

A circuit-based model for calibration of unsymmetrical non-linear (rectifying) responses of electrically-small samples in a doubly-resonant cylindrical cavity has been presented. The cavity was loaded with a support structure for testing of potentially non-linear samples and the *S*-parameter analysis of the cavity model shows that the tuned TE_{113} mode has double the resonant frequency of the TE_{111} mode, with co-located central antinodes. Any unsymmetrical non-linear behaviour in a centrally-located test sample will necessarily generate a second harmonic frequency and in order to calibrate the desired sensitivity of the detection of the produced harmonic signal, an electric circuit model was introduced and tested. By using a simulated diode connected to very short dipole arms, the non-linear response of the proposed model was established. For this rectifying element model, a non-linear relationship was demonstrated between fundamental input power and second harmonic output power. The mathematical model based on the cavity design enhances the reliability of the system as a measurement testbed that can be applied for investigation of the behaviour of biological cells or tissues (or other non-linear materials) for future applications. The diode is used as a well-characterised test-piece to prove the operational concept, although its behaviour is more extreme than might be expected in biological media, but this does not affect the validity of the calibrated electrical circuit. However, the cavity testbed can confirm the limits of any second harmonic radiation that might result from replacing the diode with biological media.

An experimental programme with a Schottky diode having variable lead lengths was also undertaken and this validated the cavity and circuital model methods, showing very good agreement with predictions. Further experimental tests underlined the effect of diode lead lengths, but, more significantly, showed the effect of immersing the diode in a small quantity of deionised water: this provided a return current path even when the diode lead lengths were minimal, thus constituting a form of distributed loop antenna. Such loop-type distributed circulating current behaviour will also be present in aqueous test samples, such as biological tissue, and can be expected to be the main coupling mechanism for such samples.

6 Acknowledgments

The authors acknowledge financial and sponsorship support from the Department of Health's Mobile Telecommunications and Health Research Programme including the Yorkshire Innovation Fund, Research Development Project and Physical Sciences *Research Council* (EPSRC) under grant EP/E022936/1, all from United Kingdom.

7 References

[1] Barnes, F., Greenebaum, B.: 'Some effects of weak magnetic fields on biological systems', *IEEE Power Electron. Mag.*, 2016, **3**, (6), pp. 60–68

[2] Vinodha, E., Raghavan, S.: 'An overview paper: possible effects of cell phone radiation'. IEEE Sponsored Second Int. Conf. On Electronics And Communication, 2015, pp. 837–841

[3] Challis, L.J.: 'Review of mechanisms for interaction between RF fields and biological tissue', *Bioelectromagnetics*, 2005, **26**, (S7), pp. S98–S106

[4] See, C.H., Abd-Alhameed, R.A., Excell, P.S.: 'Computation of electromagnetic fields in assemblages of biological cells using a modified finite difference time domain scheme', *IEEE Trans. Microw. Theory Tech.*, 2007, **55**, (9), pp. 1986–1994

[5] Ramli, K.N., Abd-Alhameed, R.A., See, C.H., *et al.*: 'Hybrid computational scheme for antenna – human body interaction'. Progress In Electromagnetics Research, PIER 133, 2013, pp. 117–136

[6] Soueid, M., Kohler, S., Carr, L., *et al.*: 'Electromagnetic analysis of an aperture modified TEM cell including an ito layer for real – time observation of biological cells exposed to microwaves'. Progress In Electromagnetics Research, PIER 149, 2014, pp. 193–204

[7] Ferikoglu, A., Cerezci, O., Kahriman, M., *et al.*: 'Electromagnetic absorption rate in a multilayer human tissue model exposed to base-station radiation using transmission line analysis', *IEEE Antennas Wirel. Propag. Lett.*, 2014, **13**, pp. 903–906

[8] Balzano, Q.: 'Proposed test for detection of nonlinear responses in biological preparations exposed to RF energy', *Bioelectromagnetics*, 2002, **23**, (4), pp. 278–287

[9] Balzano, Q., Sheppard, A.: 'RF nonlinear interactions in living cells–I: nonequilibrium thermodynamic theory', *Bioelectromagnetics*, 2003, **24**, (7), pp. 473–482

[10] Balzano, Q.: 'RF nonlinear interactions in living cells-II: detection methods for spectral signatures', *Bioelectromagnetics*, 2003, **24**, (7), pp. 483–488

[11] Balzano, Q., Hodzic, V., Gammon, R.W., *et al.*: 'A doubly resonant cavity for detection of RF demodulation by living cells', *Bioelectromagnetics*, 2008, **29**, (2), pp. 81–91

[12] Kowalczuk, C., Yarwood, G., Blackwell, R., *et al.*: 'Absence of nonlinear responses in cells and tissues exposed to RF energy at mobile phone frequencies using a doubly resonant cavity', *Bioelectromagnetics*, 2010, **31**, pp. 556–565

[13] Kowalczuk, C., Yarwood, G., Priestner, M., *et al.*: 'Nonlinear and demodulation mechanisms in biological tissue (Biological Systems)'. Final report submitted to Department of Health, 2009. Available at http://www.mthr.org.uk/research_projects/documents/RUM22bFinalReport.pdf, accessed 20 September 2016

[14] Mirza, A.F., See, C.H., Rameez, A., *et al.*: 'An active microwave system for near field imaging', *IEEE Sens. J.*, 2017, **17**, (9), pp. 2749–2758

[15] Zan, P., Yan, G., Liu, H.: 'Analysis of electromagnetic compatibility in biological tissue for novel artificial anal sphincter', *IET Sci. Meas. Technol.*, 2009, **3**, (1), pp. 22–26

[16] Martellosio, A., Pasian, M., Bozzi, M., *et al.*: '0.5–50 GHz dielectric characterisation of breast cancer tissue', *IET Sci. Meas. Technol.*, 2015, **51**, (13), pp. 974–975

[17] Breton, M., Buret, F., Krahenbuhl, L., *et al.*: 'Non-linear steady-state electrical current modeling for the electropermeabilization of biological tissue', *IEEE Trans. Magn.*, 2015, **51**, (3), p. 7402104

[18] See, C.H., Abd-Alhameed, R.A., Chung, S.W.J., *et al.*: 'The design of a resistively loaded bowtie antenna for applications in breast cancer detection systems', *IEEE Trans. Antennas Propag.*, 2012, **60**, (5), pp. 2526–2530

[19] Bottauscio, O., Chiampi, M., Zilberti, L.: 'Boundary element solution of electromagnetic and bioheat equations for the simulation of SAR and temperature increase in biological tissues', *IEEE Trans. Magn.*, 2012, **48**, (2), pp. 691–694

[20] Bahrami, H., Mirbozorgi, S.A., Rusch, L.A., *et al.*: 'Biological channel modeling and implantable UWB antenna design for neural recording systems', *IEEE Trans. Biomed. Eng.*, 2015, **62**, (1), pp. 88–98

[21] Hancock, C.P., Dharmasiri, N., White, M.*, et al.*: 'The design and development of an integrated multi-functional microwave antenna structure for biological applications', *IEEE Trans. Microw. Theory Tech.*, 2013, **61**, (5), pp. 2230–2241

[22] Scheeler, R., Kuester, E.F., Popovic, Z.: 'Sensing depth of microwave radiation for internal body temperature measurement', *IEEE Trans. Antennas Propag.*, 2014, **62**, (3), pp. 1293–1303

[23] See, C.H., Abd-Alhameed, R.A., Excell, P.S.: 'Mathematical model for calibration of nonlinear responses in biological media exposed to RF energy'. IET Computational Electromagnetics Conf. (CEM), 31 March to 1 April 2014, Imperial College London, 2014, pp. 1–2

[24] See, C.H., Abd-Alhameed, R.A., Mirza, A.F.*, et al.*: 'Mathematical model for calibration of potential detection of nonlinear responses in biological media exposed to RF energy', *Appl. Comput. Electromagn. Soc. J.*, 2017, **32**, (1), pp. 1–7

[25] CST Microwave Studio software, CST AG, Darmstadt, Germany

[26] ANSYS HFSS software, ANSYS Inc. Canonsburg PA, USA

[27] Zhao, J.X.: 'Numerical dosimetry for cells under millimetre-wave irradiation using Petri dish exposure set-ups', *Phys. Med. Biol.*, 2005, **50**, pp. 3405–3421

[28] ICNIRP: 'Guidelines for limiting exposure to time-varying electric, magnetic and electromagnetic fields (up 300 GHz)', *Health Phys.*, 1998, **56**, pp. 494–522

[29] N.R.P.B: 'Board statement on restrictions on human exposure to static and time varying electromagnetic fields and radiation', *Doc. NRPB*, 1993, **4**, pp. 7–63

[30] Keysight ADS software, Keysight Technologies, 1400 Fountaingrove Parkway, Santa Rosa, CA 95403-1799

[31] Hu, Z., Ho, V.T., Ali, A.A.*, et al.*: 'High tangential signal sensitivity GaAs planar doped barrier diodes for microwave/millimeter-wave power detector applications', *IEEE Microw. Wirel. Compon. Lett.*, 2005, **15**, (3), pp. 150–152